Analysing the Shear Behavior of Old Post-tensioned Bridges with Real Sized Beam Elements

Sebastian Lamatsch [1] ✉, *Sebastian Thoma* [2], *Oliver Fischer* [1]
✉ e-mail: sebastian.lamatsch@tum.de
[1] Technical University of Munich, TUM School of Engineering and Design, Chair of Concrete and Masonry Structures, Munich, Germany
[2] Büchting + Streit AG, Munich, Germany
DOI: https://doi.org/10.14459/icbdb24.45

Abstract The shear strength of prestressed concrete girders, especially those with limited shear reinforcement, is a subject of continuous research. Due to the lack of tests with realistic construction details and realistic heights, experimental investigations of various aspects of the shear bearing behaviour have been intensified in recent years in large collaborative research projects. This paper presents three series of experiments on different aspects of this problem. When old concrete bridges are recalculated, it is often found that their shear reinforcement is of a type that is no longer permitted. In test series 1 it is shown that they nevertheless make a significant contribution to the shear capacity. The analytical approach developed to consider them as an additive contribution is also presented. In contrast to conventional representative scaled test series, the experiments in test series 2 deliberately reduce the amount of longitudinal reinforcement to match efficiently designed bridge cross-sections and investigate the influence of longitudinal deformations on the shear capacity. Test series 3 investigates the effect of prestressing on the shear capacity with variations in the level of prestressing as well as the initial utilisation of the yield strength of the tendons on scaled cross-sections (h=1.2 m) to further analyse realistically designed beam elements. A comparison of the failure loads with the existing recalculation guideline and its forthcoming update provides further insight.

1 Introduction

The recalculation of existing bridges in Germany often results in significant deficiencies in the shear capacity check due to the constant increase in heavy traffic and adapted regulations [1], [2]. Most of the existing bridges were built between 1965 and 1985. In particular, differences in structural design and the lack of a minimum requirement for shear reinforcement lead to the deficits mentioned above. Due to the lack of tests with realistic construction details and realistic heights, experimental investigations of various aspects of the shear bearing behaviour have been intensified in recent years. Within several large joint research projects with different focuses, shear tests have been carried out on post-tensioned continuous beams with low shear reinforcement and

different cross-sectional shapes in order to draw conclusions on the load-bearing behaviour and the influence of the key parameters. The main research areas considered were

- Combined loading of shear force and torsion with predominant bending [3]
- The influence of different cross-section shapes [4]
- Contribution of non-standard stirrup types to the shear capacity [5]
- Influence of a reduced longitudinal reinforcement ratio and plastic chord deformations [6]
- Influence of the degree of prestressing in relation to concrete and prestressing steel [7]

The investigations listed are used to develop and validate modified verification formats for the recalculation guideline and its update in the BEM-ING [8][9][10].
In the following, the experimental investigations and the main results of the last three main areas of investigation, which have been carried out at the Chair of Concrete and Masonry Structures at the Technical University of Munich (TUM) in recent years, are presented. Some of the findings from the shear tests have already been directly incorporated into the recalculation guidelines, while others will be taken into account in the update of the BEM ING.

2 Experimental investigations

2.1 Substructure technique and overview of test configurations

Instead of using continuous post-tensioned concrete beams, beam elements are tested in a specially developed test rig by applying the internal forces of the selected area of a fictitious continuous beam while maintaining the compatibility of the deformations (see Figure 1). For this purpose, the desired boundary conditions are applied on the left side via six double-acting servo-hydraulic cylinders using a massive load plate (M, φ, V, w, N=0). Two vertical cylinders are mainly responsible for the vertical load vector, while the other two pairs of cylinders ensure the bending moment. There is no active control on the other side of the beam element; the rigid reaction bars on the load plate only receive the occurring internal forces and transfer them to the floor via the reaction frame. Corresponding to the reference continuous beam, this results in a linear progression of the bending moment and a constant shear force. The reinforcement and the tendons are anchored at the back of the solid load plate. In combination with shear keys for the shear force transfer and a dry pressure contact between the concrete and the load plate, this enables a force-fit connection between the beam element and the test rig. After installation in the test rig, the tendons of all beam elements are prestressed, anchored and then the duct is subsequently grouted. Further information on the test rig and its capabilities can be found here [11].

Depending on the test programme and the selected area of the reference beam, different internal forces and deformations are applied to the actively controlled load plate. For the first two configurations (old stirrup types and longitudinal deformations), the rotation at the left and right cut edges is set to zero, whereas the 1.2 m cross-section height in test series 3 requires a different cut edge to maintain reasonable shear slenderness. During the test, the required rotation is actively

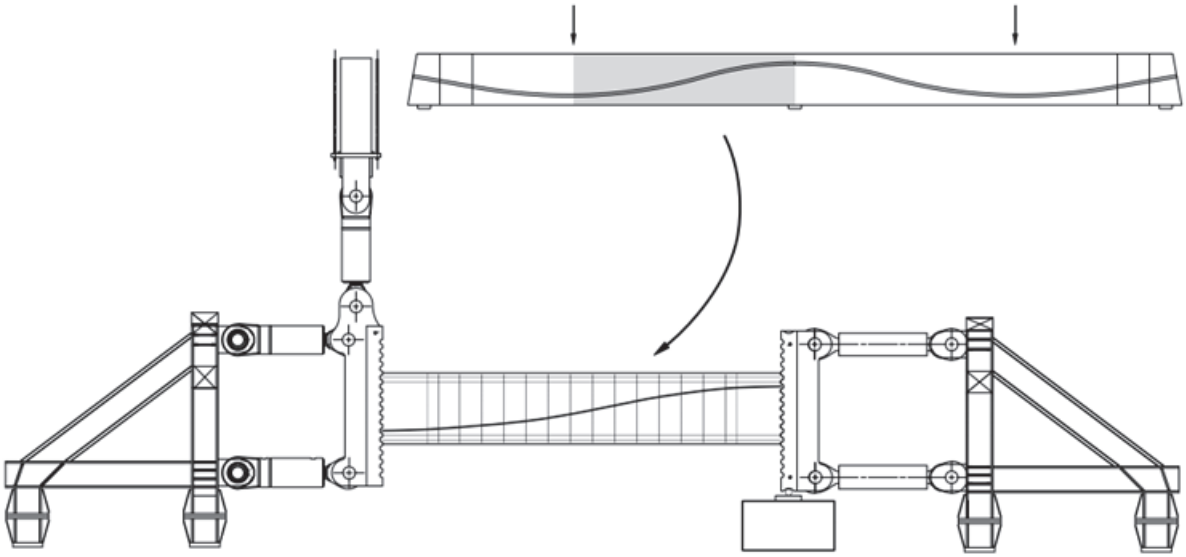

Figure 1: Test rig for testing beam elements

applied as a function of the moment-to-shear ratio on the load plate to represent the boundary conditions, thus generating an asymmetrical moment curve with a dominant negative moment. By shifting the moment zero point, only the failure in the area of the inner support of a prestressed continuous girder is tested, which is often decisive for old prestressed concrete bridges.

Figure 2 gives an overview of the different configurations of all 3 test series. In the following chapters, the ID of each specimen already provides the most important information on the parameters investigated. A distinction is made between the cross-sectional shape (rectangular/T-cross-section) and the diameter of the longitudinal reinforcement, as well as the number of strands (L3/L5/L9) and the concrete compressive stress from prestressing (S1.2 = 1.2 MPa). If special stirrups are present, the stirrup shape of the first test series is indicated using abbreviations such as closed stirrups (cs), open stirrups (os), with additional open stirrups (aos) and stirrups with short lap length (ll).

2.2 Contribution of non-standard stirrup types to the shear capacity

Existing concrete bridges often have stirrup types that are no longer permitted by current codes and therefore cannot be used in the shear capacity check. Therefore, this circumstance is taken into account in the series of tests presented in extracts. In addition to two reference tests without and two with conventional closed stirrups, outdated stirrup types were tested. With that, it was possible to formulate an analytical model to properly consider the shear capacity of these stirrups.

Test program

The influence of outdated stirrup types is the focus of the excerpt from the test series presented here. For each configuration, two tests are carried out with the same design. A distinction is made between closed stirrups, stirrups open at the top, closed stirrups with additional stirrups open at the top in the area of negative bending moments and two-part stirrups with a short overlap length. A further test with increased shear reinforcement is not shown. Comparison of the tests

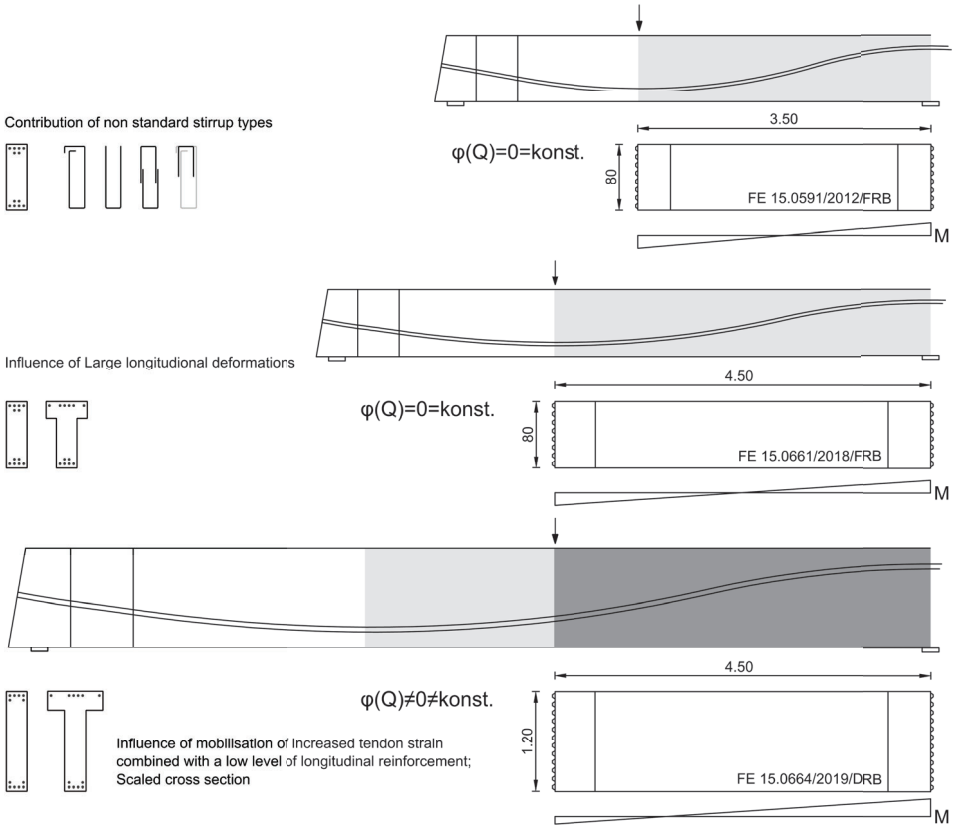

Figure 2: Test setups of the three presented test series.

with the old stirrup shapes with the reference tests without and with conventional stirrups gives an indication of the capacity of each stirrup type. All beam elements are 3.5 m long, 80 cm high, have the same longitudinal reinforcement ratio of 1.59% and a prestress of 2.5 MPa. Further test data is given in Table 1.

Table 1: Distinctive features, concrete properties and shear failure loads of the presented beam elements

ID	Stirrup type	$f_{c,cyl}$ [MPa]	$f_{ct,sp}$ [MPa]	E_{cm} [MPa]	V_{max} [kN]
R1	No stirrups	41.9	3.4	31 849	596
R2-cs	Ø6/25cm closed stirrups	47.0	3.8	33 777	711
R3-cs	Ø6/25cm closed stirrups	48.1	4.1	34 037	713
R4-os	Ø6/25cm open stirrups (tcp)	37.6	3.3	33 130	659
R5-os	Ø6/25cm open stirrups (tcp)	45.6	3.3	33 988	583
R6-aos	cs + Ø6/25cm additional open stirrups (top) at neg. moments	40.8	3.3	34 037	704
R7-aos	cs + Ø6/25cm additional open stirrups (top) at neg. moments	38.8	2.8	32 864	668
R8-ll	Ø6/25cm two-part stirrup with short lap length	44.4	3.4	33 137	704
R9-ll	Ø6/25cm two-part stirrup with short lap length	38.7	3.4	33 847	661
R10	No stirrups	43.4	3.3	33 357	596

Characteristic load-bearing behaviour

In all test beams with shear reinforcement, the stirrup reinforcement along the critical shear

crack reached its yield strain before failure. The increasing mobilisation of the existing shear reinforcement delayed the propagation of the critical shear crack into the compression zone, but after pronounced shear cracking and yielding of the stirrups, shear failure occurred due to propagation of the critical shear crack into the compression zone, depending on the degree of stirrup reinforcement and the design of the stirrups. Failure of all beams was preceded by a further increase in load after the early onset of cracking (40-60 % Vmax) and can therefore be classified as generally ductile, although the ultimate failure was brittle.

Main results

The contribution of old stirrup types to the shear capacity depends significantly on the anchorage length and the location of the critical shear crack. The position of the anchorage in the beam has an important effect, as a compression chord anchorage, for example, ensures significantly better force transfer. Fiber-optical strain measurements along the stirrup legs have shown that with two-part stirrups, even a very short overlap length in the range of 1/3 of the length required by EC2 [12] is sufficient to reach 80 % to 100 % of the yield strength of the stirrups when shear cracking occurs, thus significantly increasing the shear capacity. However, when anchoring straight bar ends of open stirrups, shear cracking leads to a shortened anchorage length and thus also to a reduced force transfer (see Figure 3). Depending on the expected shear cracking and any existing compression chord, considerable previously unconsidered load-bearing components can therefore be used, depending on the position and shape of the respective stirrup.

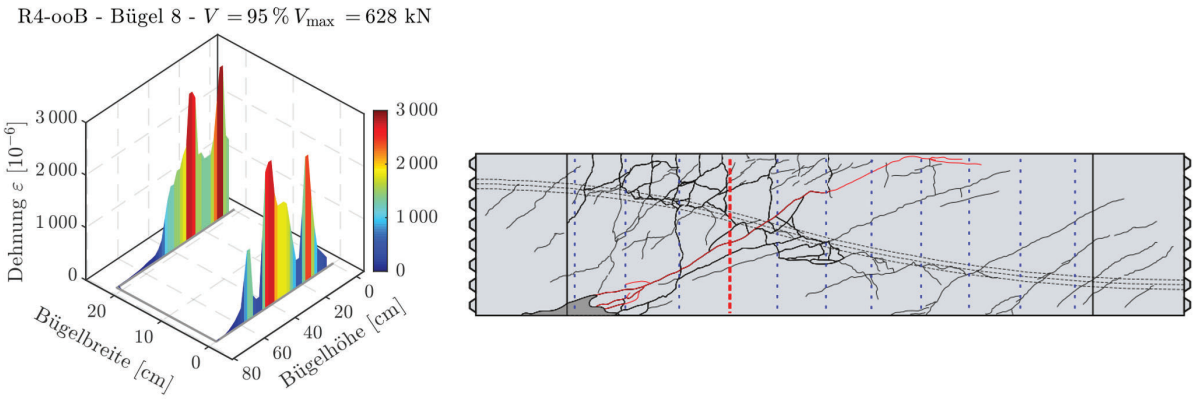

Figure 3: Strain measurement on an open stirrup and location in the beam element [11]

Simplified analytical consideration of outdated stirrup types

In [11], a simplified approach was developed for arbitrary integration of the contribution of old stirrup types to the shear capacity, based on the well-known truss model. The crack angle and the strut angle are set equal and the crack is idealised by a discrete crack with an idealised inclination β_r. The angle β_r is defined by equation 1 as described in [13].1

$$\cot \beta_r = 1.2 + \frac{f_{ck}}{150 \rho_w f_{yk}} - 2.4 \cdot \sigma_{cp} / f_{ck} \leq 2.25 \tag{1}$$

The projected horizontal length ($z \cdot \cot \beta_r$) represents the area of the stirrups to be considered

for closed stirrups because the yield strength is reached as a result of good anchorage. Due to the different bond conditions of the old stirrup shapes, not all stirrups crossed by the shear crack can be fully considered. Therefore, z is reduced by the anchorage length or lap length of the stirrup legs. This ultimately results in a shorter horizontal length $z_{mod} \cdot \cot \beta_r$ to account for the stirrup reinforcement in the respective design section (see Figure 4). The same applies to two-piece stirrups with too short lap length. The positive effect of a stirrup anchorage in the compression chord can also be taken into account. The additive component of non-standard stirrups is then calculated according to equation 2.

$$V_{Rd,sy,ad} = a_{sw} \cdot z_{mod} \cdot f_{yd} \cdot \cot \beta_r \tag{2}$$

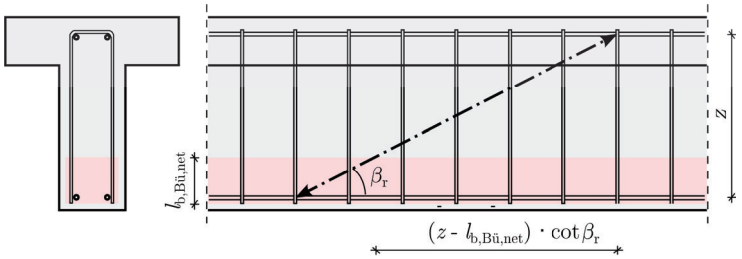

Figure 4: Calculation of the stirrup contribution of open stirrups with no possible consideration of the positive effect of a compression chord [11]

2.3 Influence of a reduced longitudinal reinforcement ratio and plastic chord deformations

In shear tests carried out to date, a very high degree of longitudinal reinforcement has been found almost exclusively, which should rule out early flexural failure in favour of shear failure. A series of tests, parts of which are presented here, investigates the influence of a successively reduced degree of longitudinal reinforcement, which better reflects the possible high longitudinal deformation of economically designed bridges.

Test program

Eight tests on beam elements are used to investigate the influence of longitudinal reinforcement on the shear capacity of old prestressed bridges. Three different levels of bending reinforcement with ribbed reinforcing steel are investigated on beams with rectangular and T-sections. All other parameters remain identical and can be found in Table 2. The tests on T-beams allow conclusions to be drawn about the contribution of the chords, which can also be seen in relation to the stiffness of the tension chord. The length of the beam element is 4.5 m with a height of 80 cm. An additional test for each cross-section with smooth longitudinal reinforcement is not discussed further in this article. As the analysis of old bridges is of interest, the beams are designed with approximately the minimum shear reinforcement as calculated by [8].

Characteristic load-bearing behaviour

In all tests of the series, a classic flexural shear failure was achieved despite the low longitudinal

Table 2: Distinctive features, concrete properties and shear failure loads of the presented beam elements

ID	ρ_{sl} [-] (abs.)	$f_{c,cyl}$ [MPa]	$f_{ct,sp}$ [MPa]	E_{cm} [MPa]	V_{max} [kN]
R25	0.016 (6D25)	41.9	3.03	28 810	484
R22	0.012 (6D22)	40.3	3.04	29 480	517
R18	0.008 (6D18)	44.4	3.04	28 630	585
T25	0.016 (6D25)	41.9	3.54	27 960	510
T22	0.012 (6D22)	53.7	3.67	31 260	609
T18	0.008 (6D18)	43.8	3.84	28 590	579

reinforcement ratio. Under severe crack opening, the shear reinforcement breaks and the compression zone narrows. However, before the ultimate load is reached, the T-beam, in particular, also increasingly shows direct shear tension cracks in already cracked compressive stress fields in the span and support areas. When the ultimate shear capacity is reached, the final crack kinematics are localised in a critical flexural shear crack or in a diagonal shear crack. The energy released can only be absorbed by the stiffness of the chords or the crossing tendon, which is why the failure of the tests with the lowest level of longitudinal reinforcement is particularly abrupt.

Main results

In the series of tests analysed, a reduced ratio of longitudinal reinforcement does not have a negative effect on the shear capacity. Despite the significantly reduced longitudinal reinforcement ratio and the partial plastic deformation of the reinforcement in the tension chord, the internal equilibrium of the horizontal forces can be maintained by the initially moderately prestressed tendons, so that a sufficient bending resistance in favour of a primary shear failure can be ensured, see Figure 5. Due to the low degree of stirrup reinforcement, the deformations of the tension chord control the development of the crack widths of the shear cracks and thus determine the steel stress or the early rupture of the stirrups based on the compatibility of the deformations in the crack, which could be observed several times during the experimental investigations.

As soon as flat shear cracks start to form in the shear section, the system reaches the ultimate load because the stirrups, with such a low level of reinforcement and such a small diameter, cannot have a crack-limiting effect. Therefore after initial activation, steel stresses above the yield point are directly induced, followed by stirrup rupture, which triggers the final crack kinematics.

2.4 Influence of different levels of post-tension and residual tendon strain

Experimental investigations of the shear capacity of old post-tensioned concrete bridges in recent years have already covered a large number of influencing parameters, but less attention has been paid to the influence of the mobilised tendon strain and its influence, if limited. Most of the documented tests have also been carried out on girders with a maximum height of 80 cm, so that for the first time significantly scaled realistically designed cross-sections are being tested. The series of tests presented in extracts focuses on these aspects in connection with the general realistic design of old bridge structures.

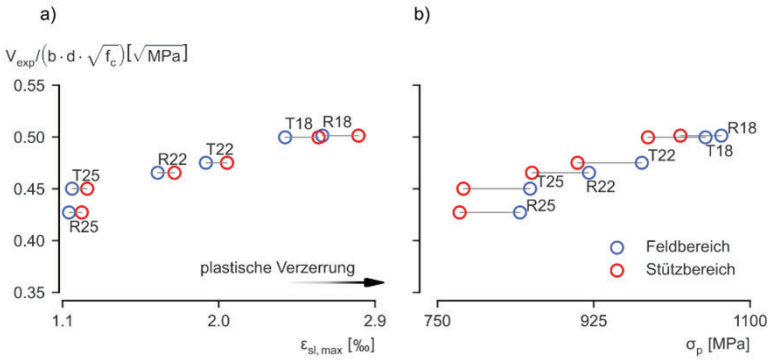

Figure 5: Normed shear capacity compared to a) maximal deformations of the longitudinal reinforcement and b) maximal tendon strain at the cut of the widening at negative and positive moment sections.

Test program

In the part of the test series presented here, the influence of prestressing on the shear capacity is investigated in a differentiated manner using eight beam elements. On the one hand, the influence of increased concrete compressive stresses is investigated by varying the absolute prestressing force. On the other hand, the number of strands is varied in order to test a moderate and a high initial utilisation of the tendon. The selected low degree of longitudinal reinforcement, which is based on real bridge conditions, leads to a large mobilisation of the strain reserves in the tendon and allows the investigation of redistributions between reinforcement and tendon. Corresponding to old bridges, both the rectangular and the T-beams are designed in the range of 1.0 times the minimum shear reinforcement ratio. The maximum shear capacity and a list of the most important parameters of each test are shown in Table 1.

Table 3: Extract from the test series, variation of prestressing, concrete parameters and maximum shear capacity

ID	$\sigma_{pm0}/f_{p0,1k}$ [-]	σ_{cp} [MPa]	$f_{c,cyl}$ [MPa]	$f_{ct,sp}$ [MPa]	E_{cm} [MPa]	V_{max} [kN]
R-L5-S1.7	0.44	1.78	42.6	3.6	30 049	775
R-L3-S1.7	0.72	1.76	46.2	3.8	30 157	829
R-L9-S3.1	0.42	3.06	43.7	3.5	27 999	927
R-L5-S3.1	0.74	3.00	43.3	2.8	27 991	982
T-L5-S1.2	0.41	1.15	47.6	3.2	29 727	862
T-L3-S1.2	0.60	1.02	50.4	3.3	30 361	776
T-L9-S2.1	0.36	1.82	48.4	3.8	29 721	971
T-L5-S2.1	0.68	1.90	47.7	3.2	29 641	902

Characteristic load-bearing behaviour

In all tests - despite a very high longitudinal strain of at least 80 % of the yield strength of the bending reinforcement - a classical flexural shear failure was observed. The load-bearing behaviour was characterised by strong crack kinematics and significant involvement of the tension chord. Starting with fan-shaped flexural shear cracks, yielding stirrups and isolated tension cracks in the web, especially in the T-beams, the compression zone narrows and fails in combination with the rupture of almost all stirrups crossing the critical shear crack. Due to the low degree of

longitudinal reinforcement and the generally realistic design of a comparable bridge girder, the tendon contributes significantly to the load transfer even with initially high strain in the tendon and additional local and global strain growth and, depending on the crack geometry, does not impair the load-bearing behaviour.

Main results

An initial high strain in the tendon does not necessarily lead to a reduction in shear capacity in the tests carried out. Depending on the shape of the cross-section, further redistributions are possible despite a highly stressed tendon. The necessary compatibility of the deformations of the tension chord and the web thus significantly determines the overall load-bearing behaviour, resulting in a different crack pattern due to the connected plate of the T-beam and the different prestressing. The crack pattern of two exemplary tests with a rectangular cross-section and different concrete compressive stresses due to prestressing is shown in Figure 6a) together with the strain profile of a robust fibre optic sensor (DFOS) laid in the duct. The strains occurring after the start of loading are plotted perpendicular to the tendon. The local strain increase due to shear cracking is clearly distinguishable from the global increase due to bending at the intersections with the tendon. Overall, there is good agreement between the strain measurement and the recorded crack pattern. The positive influence of the prestressing on the associated load-bearing capacity, which is evident in all tests, is shown in Figure 6b) - with the initial vertical prestressing force subtracted.

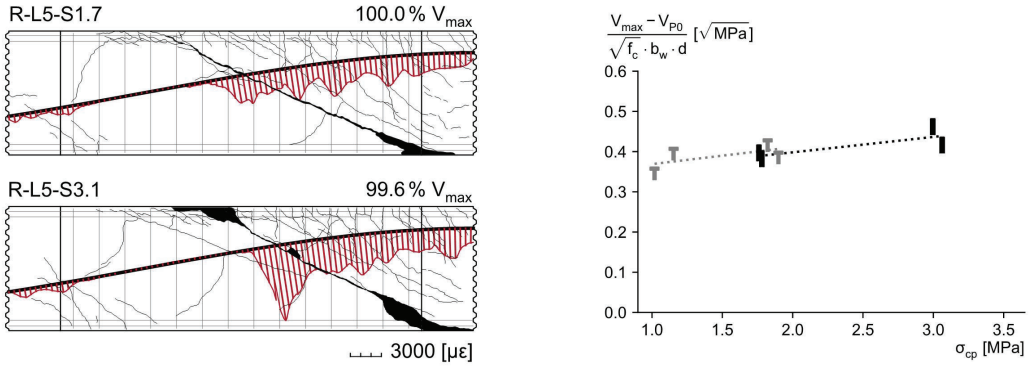

a) Crack pattern of two beam elements with strain profile of the tendons

b) Influence of the prestressing on the normed shear capacity

Figure 6: Influence of prestressing on crack formation, tendon strain in the crack and shear capacity

3 Comparison to analytical models

Figure 7 shows a comparison of tests from all three research projects with models for the recalculation of bridges in Germany. Only tests with ribbed bars and low degree of shear reinforcement are shown. The calculated shear capacities with the 2015 recalculation guideline model show very poor agreement with the test data. The further development of the recalculation guideline, which will be applicable in Germany in 2025 within the BEM ING, shows a much better agreement. This is due to an additional concrete contribution to the shear capacity, which is particularly relevant

for old bridges with little shear reinforcement. It can be seen that there are still residual capacities due to higher prestressing, the cross-section of the T-beams and low levels of longitudinal reinforcement.

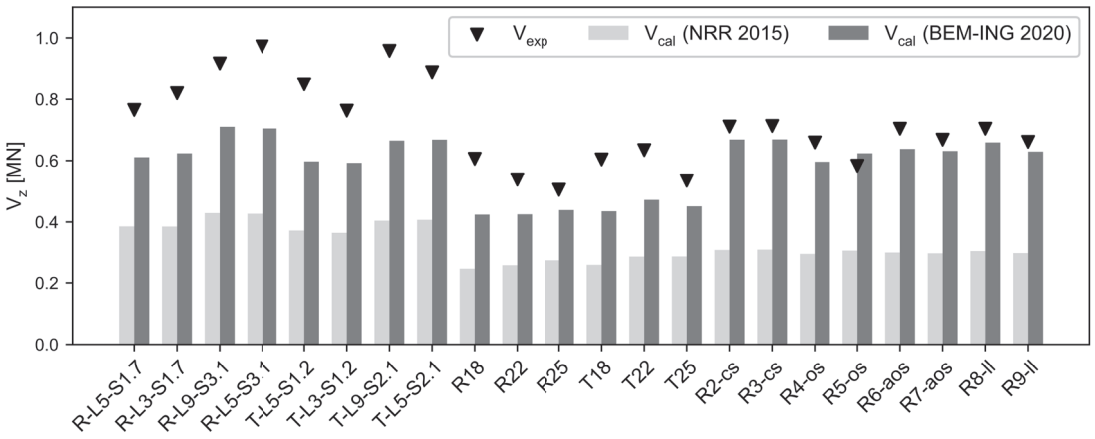

Figure 7: Comparison of analytical approximations and the experimental shear capacity

4 Conclusion

The test series showed that old stirrup shapes, despite poor anchorage with straight legs, participate in shear force transfer and contribute to the shear capacity depending on the bond conditions. The development of a simplified engineering model, which takes into account the contributing stirrups depending on their shape and anchorage, can now help to successfully recalculate old bridges with stirrup shapes that could not previously be taken into account. Even a very high utilisation of the longitudinal reinforcement, due to the progressively lowered longitudinal reinforcement and initially highly utilised prestressing strands, does not adversely affect the load-bearing behaviour. Overall, the use of realistically scaled cross-sections with realistic system boundary conditions has enabled the test data from relevant shear tests to be extended and the understanding to be improved. The work presented here fills a number of important gaps, as the parameters have not yet been investigated experimentally, or have only been investigated on small, unrealistic test beams. On the basis of a truss model with an additional concrete component and the additional consideration of no longer standardised stirrup shapes, large reserves of load-bearing capacity can already be utilised in many cases. This makes it possible to recalculate old prestressed bridges more realistically without much effort, thus delaying the strengthening or demolition.

5 References

[1] Nowak, M.; Fischer, O.: Objektspezifische Verkehrslastansätze für Straßenbrücken – ein wichtiger Baustein für erweiterte Beurteilungskonzepte in der Brückennachrechnung. In: Beton- und Stahlbetonbau 112 (2017), Heft 12, S. 804–814. https://doi.org/10.1002/best.201700064

[2] Fischer, O.; Müller, A.; Lechner, T. et.al.: Ergebnisse und Erkenntnisse zu durchgeführten Nachrechnungen von Betonbrücken in Deutschland. In: Beton- und Stahlbetonbau 109 (2014), Nr. 2, S. 107–127. https://doi.org/10.1002/best.201300084

[3] Gleich, P.; Maurer, R.: Arch Action Model for the structural assessment of existing prestressed concrete bridges . Structural Concrete. 2023; 24(5): 5827–5838. https://doi.org/10.1002/suco.202201008

[4] Herbrand, M.; Adam, V.; Hegger, J.: Shear Tests on Prestressed Concrete Continuous Beams. In: ACI SP-333: Advances in Concrete Bridges: Design, Construction, Evaluation, and Rehabilitation 1 (2019), Chapter 7

[5] Schramm, N.; Fischer, O.: Zur Anrechenbarkeit von nicht norm-gemäßen Bügelformen auf die Querkrafttragfähigkeit von Bestandsbrücken. In: Bauingenieur. 95 (2020); Heft 11, S. 408 418. https://doi.org/10.37544/0005-6650-2020-11

[6] Thoma, S; Fischer, O.: Experimental investigations on the shear strength of prestressed beam elements with a focus on the analysis of crack kinematics. Structural Concrete. 2023. https://doi.org/10.1002/suco.202200699

[7] Lamatsch, S.; Fischer, O.: Querkraftversuche an unterschiedlich hoch vorgespannten Balkenelementen mit baupraktischen Bauteilabmessungen/ Experimental investigations on the shear strength of prestressed beam elements with realistic dimensions and varying degree of prestressing. In: Bauingenieur 99 (2024), Heft 01-02, S. 35-45, doi.org/10.37544/0005-6650-2024-01-02-57

[8] Bundesministerium für Verkehr, Bau und Stadtentwicklung (BMVBS): Richtlinie zur Nachrechnung von Straßenbrücken im Bestand (Nachrechnungsrichtlinie). Berlin, Mai 2011.

[9] Bundesministerium für Verkehr und digitale Infrastruktur (BMVI): 1. Ergänzung zur Richtlinie zur Nachrechnung von Straßenbrücken im Bestand (Nachrechnungsrichtlinie). Berlin, April 2015

[10] Bundesministerium für Verkehr und digitale Infrastruktur (BMVI): Teil 2 - Nachrechnung von Straßenbrücken im Bestand: (in Vorbereitung). In: Regelungen und Richtlinien für die Berechnung und Bemessung von Ingenieurbauten (BEM-ING) Entwurf, Bonn, 2020.

[11] Schramm, N.: Zur Querkrafttragfähigkeit von Spannbetonbalkenelementen unter besonderer Berücksichtigung der Bügelform, Technical University of Munich (TUM), Dissertation, 2021, https://mediatum.ub.tum.de/1601310

[12] Eurocode 2: Design of concrete structures - Part 2: Concrete bridges - Design and detailing rules, European Committee for Standardization. 2010.

[13] Herbrand, M.: Shear strength models for reinforced and prestressed concrete members, RWTH Aachen University, Dissertation, 2017. https://doi.org/10.18154/rwth-2017-06170